Unit 1 Steam Turbine Generator of Noshiro Thermal Power Plant, Tohoku Electric Power Co., Inc.

Shozo Yagoh
Takashi Kobaru
Tadao Suzuki

1. Introduction

Unit 1 of Noshiro Termal Power Plant, Tohoku Electric Power Co., Inc., is a tandem compound machine. The capacity of this generator belongs to the maximum class of 50Hz thermal power machines in Japan. The safety of each part of an enlarged rotor and high electric loading is important to the reliability of a large capacity machine. It is also important for the generator to have a high rate of efficiency.

The features of Unit 1 Steam Turbine Generator of Noshiro Thermal Power Plant are introduced in this paper. In addition, the technology utilized to improve reliability and attain higher efficiency of this generator is described with the use of verification and testing results. The intended merit of this generator and exciter is the simplification of operation and maintenance. We believe that direct hydrogen-cooling and a brushless exciting system applied to the generator and exciter are very effective in achieving this merit.

2. Specifications and parameters

Table 1 shows the main specifications and parameters of the generator, exciter and sub-exciter.

Figure 1 shows a cross section of the 670 MVA generator.

Table 1 Specifications of generator

Generator	Capacity	670MVA
	Voltage	19,000V
	Power factor	0.9
	Frequency	50Hz
	Cooling method	Stator winding; direct-cooled by hydrogen Rotor winding; direct-cooled by hydrogen
	Hydrogen gas pressure	4.0 bar (400kPa), gauge pressure
	Rotational speed	3,000r/min
	Short circuit ratio	0.58
	Exciting	Brushless exciting
Brushless exciter	Capacity	3,780kW
	Voltage	600V (DC)
	Current	6,300A (DC)
	Number of diodes	120
	Diode connection	3-Phase bridge connection
Sub-exciter	Type	Permanent magnet generator
	Capacity	65kVA
	Voltage	220V
	Frequency	400Hz
Total length		17.7m
Total mass		553t
Mass of stator for lifting		345t
Mass of rotor		68t

3. Merits of the generator

3.1 Cooling system

The stator and rotor windings are cooled directly by hydrogen. This system has the advantage of making maintenance significantly easier as compared with water-cooling (which requires two types of coolant) because there is no need for the auxiliary equipment or the provisions for operation monitoring, which are required when the windings are water cooled.

The capacity of the generator's direct hydrogen-cooling system is 850 MVA under present conditions and it is planned to expand it to 1,000 MVA, a realizable goal. The capacity of this generator is well within this range.

Figure 2 shows the cooling path in the generator. This cooling path consists of the following:

(1) Path I: The rotor winding of the turbine side is cooled.
(2) Path II: The stator core (including the core's end zone on the turbine side) is cooled.
(3) Path III: The stator winding, rotor winding of exciter side, end of stator core of exciter side and bushings are cooled.

In these paths, the distribution of necessary gas flow rates is set according to the generated loss of each part, and orifices of each part are adjusted so that the gas flow rates reach the predetermined values of the shop test. **Table 2** shows the distribution of generated losses and gas flow rates in the generator's gas passageway.

3.2 Cooling at the end zone of the core

Since stray load loss caused by leakage flux at the end

Fig. 1 Cross section of 670MVA generator

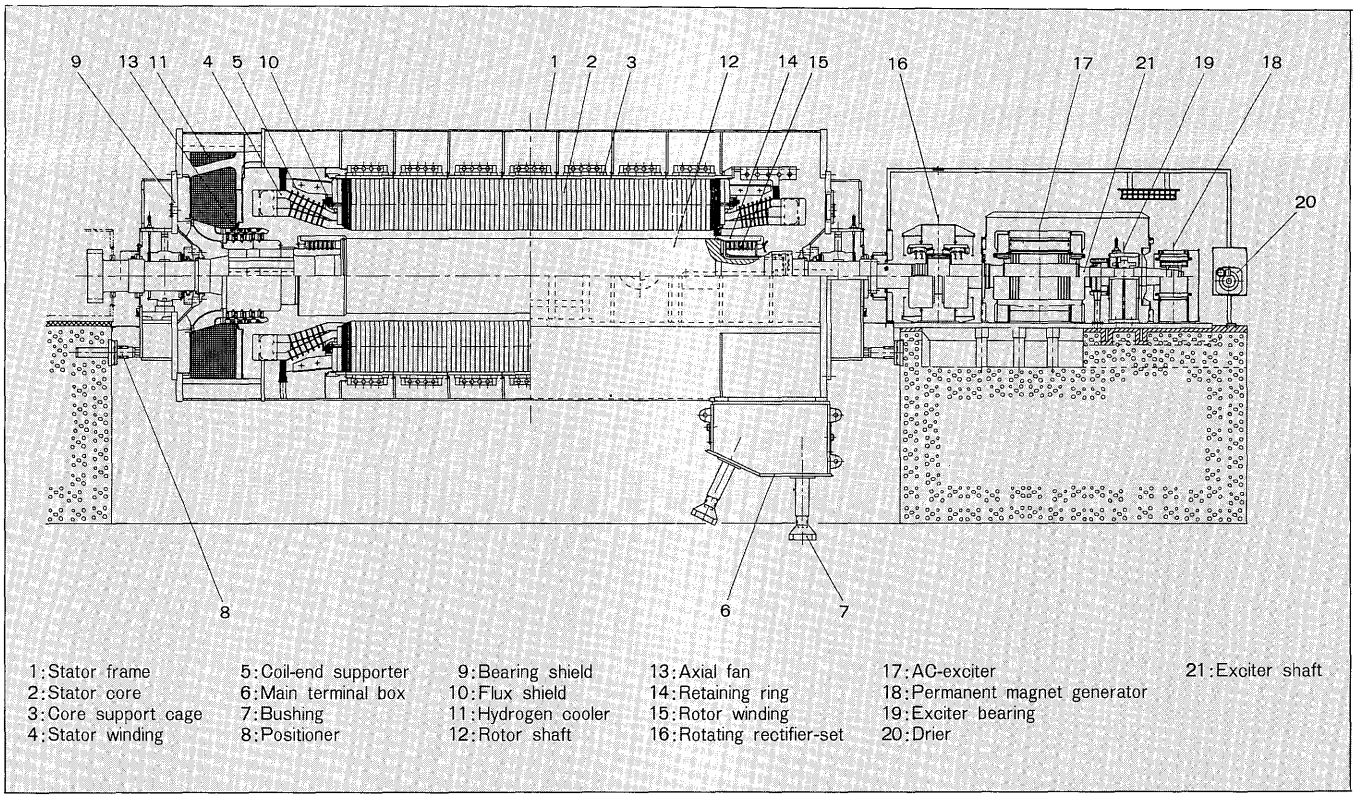

Fig. 2 Ventilation of generator

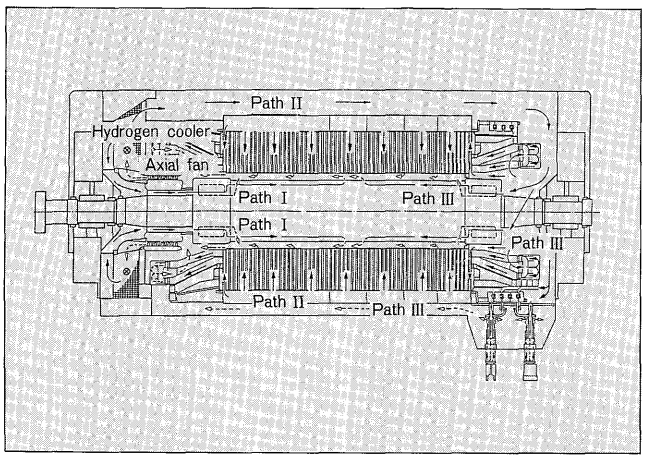

Table 2 Losses and distribution of coolant

Cooling path	Components	Generation of loss	Distribution of coolant
Path I	Rotor winding (first side of two)	15%	15%
Path II	Surface of stator core and rotor body	30%	38%
	Flux shield and press-ring		
	Core end		
Path III	Stator winding	40%	47%
	Rotor winding (second side of two)		
	Flux shield and press-ring		
	Core end		
	Bushing		
Fan		15%	–

of the stator is increased in a large turbogenerator as electric loading is increased, thorough consideration is necessary to decrease the loss and prevent overheating. Various countermeasures adopted for this generator are shown in **Table 3**. **Figure 3** shows details of the core's end zone. The cold gas after the cooler is guided from the outer side of the iron core, flowing directly to a subdivided core of 10+ mm thickness and a flux shield, where powerful cooling occurs. The purpose of increasing the gas quantities in paths II and III compared with the generated losses in the above **Table 2** is to emphatically distribute gas quantities to the end zone of the stator core.

3.3 Stator winding

Figure 4 shows the cross section of the stator winding. Roebel-transposition is applied to strands of the coil. Moreover, a section of coil with a different strand configuration is adopted for the upper and lower coils, thus decreasing loss. This relationship between coil loss to thickness is shown in **Fig. 5**. The tendency is that skin-effect-loss increases as the thickness of the strand in the upper coil increases; strand configuration is selected in order to minimize total coil losses (skin-effect-losses + Joule-losses).

As the insulation of the winding causes aging, diligent

Table 3 Measures for cooling at core end

Item	Measures	
Reduction of losses	Stator	Flux shield of stacked core
		Slitted core-teeth
		Stepped core end
	Rotor	Non-magnetic retaining ring
		Longer rotor body than stator core
Improvement of cooling effect	Adequate coolant flow at end core portion	
	Adequate cooling surface at end core portion by subdividing core laminated block	
Monitoring of temperature	Measuring at the highest point	
Control in manufacturing	Removal of burr of punched core plate, Varnish treatment Core test	

Fig. 3 Cooling of stator core end

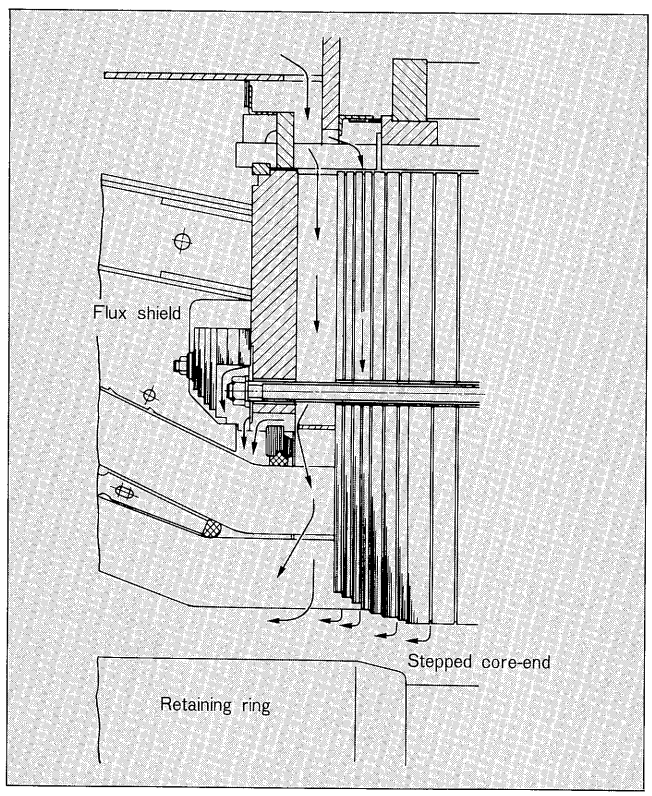

Fig. 4 Slot of stator and rotor

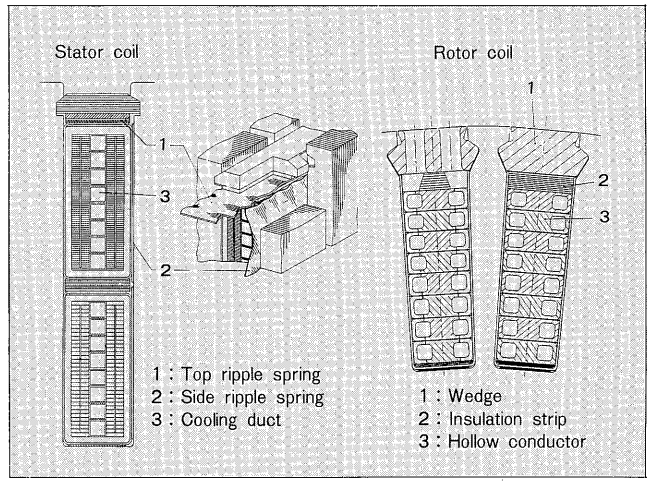

Fig. 5 Loss of coil vs. thickness of strand

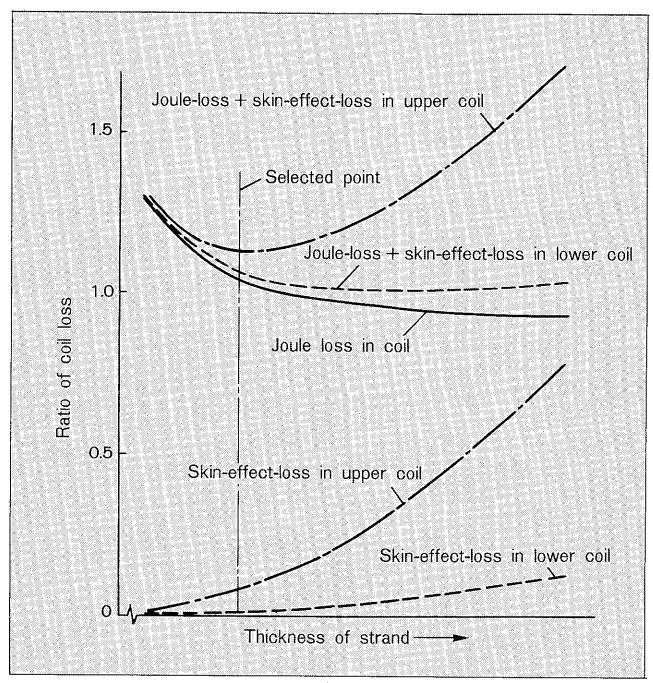

maintenance is conventionally needed to prevent the coil from loosening. Since the loosened coil vibrates in the slot, mechanical or electrical damage such as vibration-spark is caused. A top ripple spring shown in **Fig. 4** is a preventive countermeasure for the coil which fixes the coil in the slot with a spring strength of several times the electro-magnetic force. Moreover, a side ripple spring makes the coil stick to the slot wall, suppressing vibration and securely grounding the coil surface.

Furthermore, after aging of the insulation in this generator was accelerated in the workshop, deformation decreased as shown in **Fig. 6** As for the forced aging of the insulation, the coils are heat pressed in the slot using a temporary wedge and pressing tube as shown in **Fig. 7**.

Because of this, maintenance is greatly reduced.

3.4 Rotor

(1) Form optimization of rotor slot

In this generator, the shape of the rotor slot was improved. That is, by cooperating the electrical design (ampere-turn, flux density, temperature rise of winding) and the mechanical design (each part of slot, wedge stress, etc.), the optimization was pursued as a whole and is shown in the above-mentioned **Fig. 4**. As a result, the slot depth became 15% shallower and the mechanical loads of the wedge and retaining ring decreased by about 10%, as compared with that of a conventional design. On the other hand, it was confirmed by the shop test that the no-load saturation characteristic and the 3 phase short circuit characteristic were as predicted, which will be described later.

Fig. 6 Forced aging of insulation in stator slot

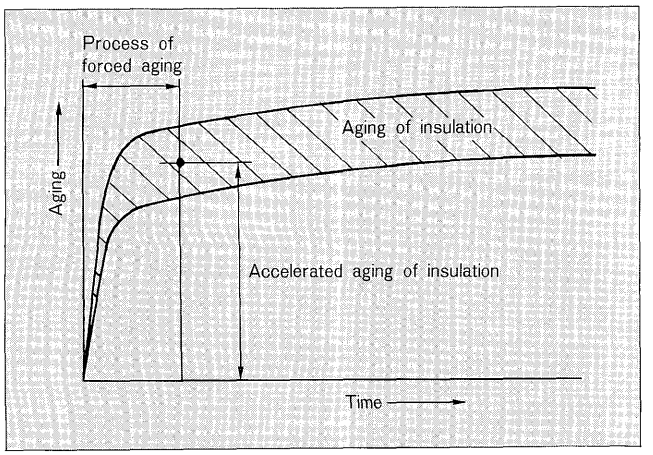

Fig. 7 Aging process of stator winding

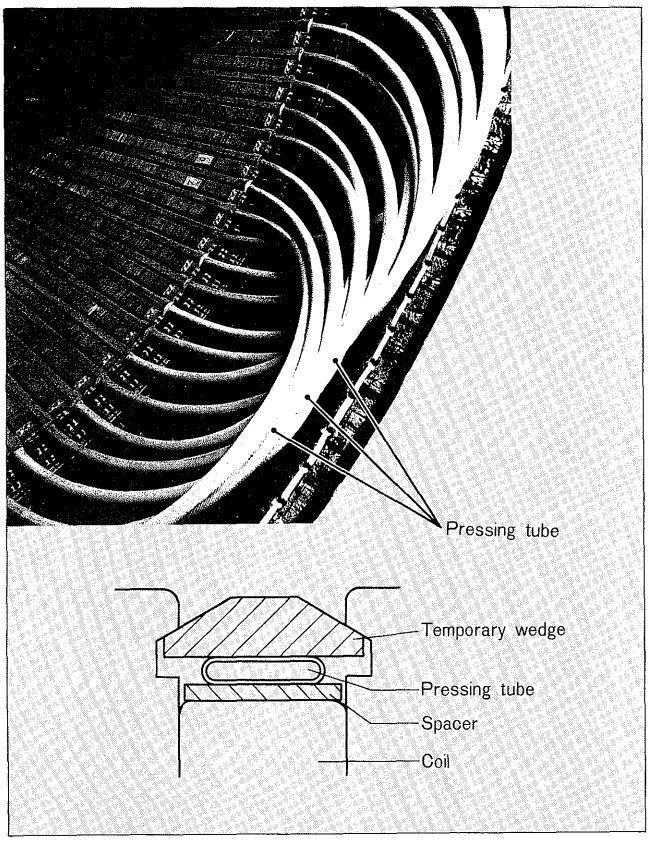

Fig. 8 Unequal temperature and rotor deformation

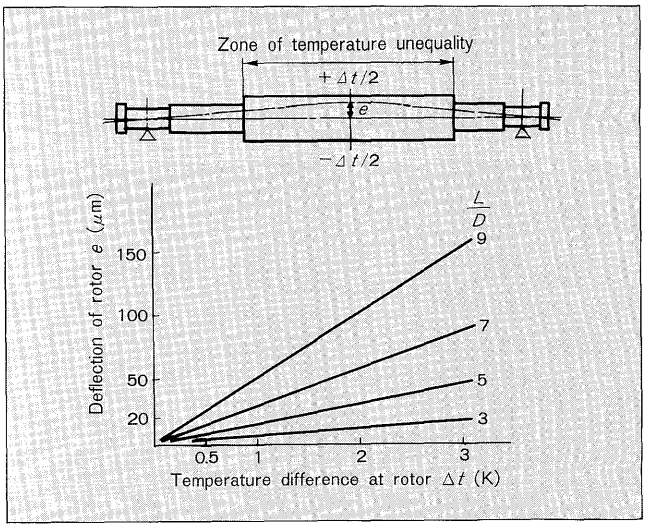

Fig. 9 High response exciting to ceiling

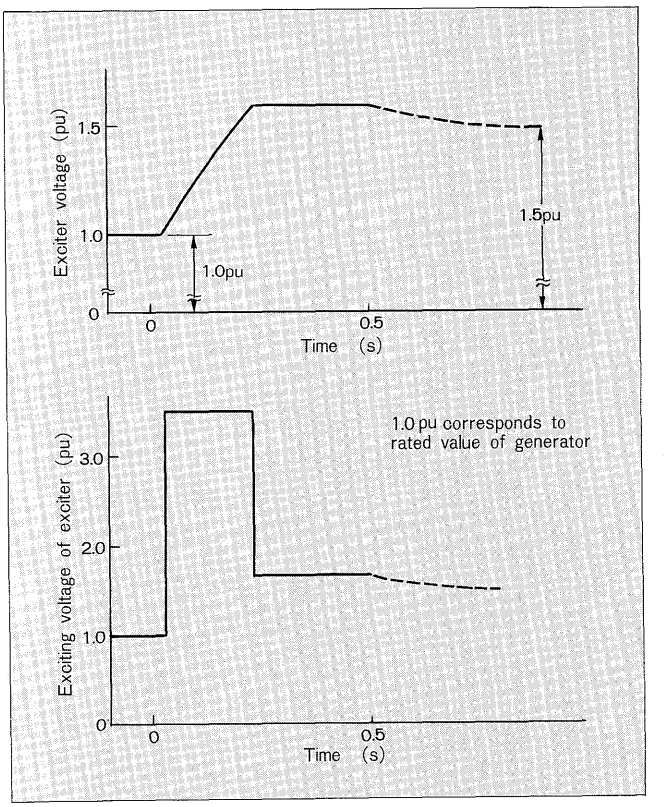

(2) Thermal imbalance

The rotor becomes longer and larger as generator output increases. When the degree of size is expressed with the length/diameter ratio L/D, which represents the ratio of the rotor core length (L) and diameter (D), Fuji Electric believes that L/D is limited to about 7, because of restrictions such as the increase of imbalance sensitivity and the decrease of bearing stability due to a decline in critical speed. The L/D of this generator's rotor is 5.1 and has not yet reached the limiting value. However, this is the maximum value as a turbogenerator made by Fuji Electric. The tendency of thermal imbalance is thought to be important in the restriction factor of L/D, as shown in **Fig. 8**. For instance, it is understood to cause an imbalance which cannot be disregarded even if a temperature discrepancy of about 1 K exists between the opposite points on the rotor circumference.

Countermeasures to decrease thermal imbalance are detailed in another report[1].

3.5 Brushless exciter

This exciter is the greatest of the 3,000 min^{-1} machines in Japan. In addition to the main AC-exciter and

rotating rectifier-set, which comprise the system, a permanent magnet generator is installed as a sub-exciter on the same shaft, supplying stable exciting power to the main AC-exciter in the event of a voltage drop due to a system accident.

In this generator, in order to increase exciter response, the time constant must be reduced. To accomplish this, the air gap is wider than in a conventional exciter and a damper winding is not installed in the magnetic poles. Moreover, as shown in **Fig. 9**, to increase the exciter voltage, exciting voltage of 3.5 pu is applied to the exciter field in the first step. When the field current of the exciter reaches a predetermined value, the exciting voltage is returned to 1.5 pu. Although exciter response is achieved at around $1.9s^{-1}$, this brushless exciter system is evaluated as having a high response ratio.

Table 4 Computer aided monitoring

Monitoring item	Monitoring
Stator winding temp.	Compare and analyze measured value and the value calculated according to generator load
Stator core end temp.	
Rotor winding temp.	Value according to generator load
Failure of exciter diode	Detect failure of phase
Operating conditions	Indicated by diagrams on CRT See/Fig. 10
Hydrogen gas consumption	Consumption value calculated from change of gas pressure in generator

Fig. 10 CRT-display, generator operating point

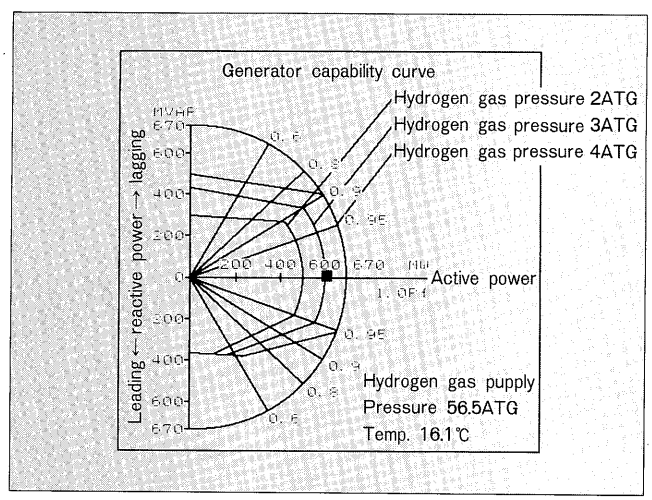

Fig. 11 No-load saturation curve and three-phase short circuit curve

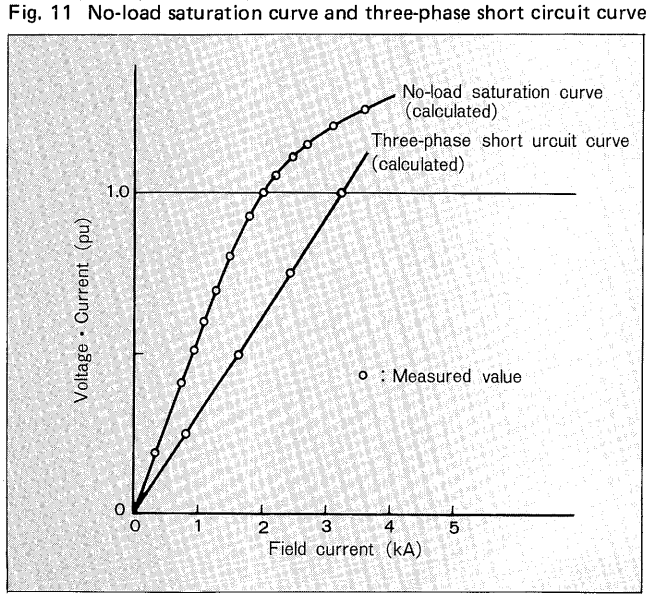

3.6 Operation monitoring

The computer is widely used for operational monitoring of the generator. **Table 4** shows the features of computer-aided monitoring.

Since the generator has the brushless exciter system, the rotor winding temperature shown in this table covers the impossibility of directly monitoring the rise in rotor temperature. The error between the computer's temperature value output and the measured temperature rise is within 0.5%.

An example of the generator's operating point displayed on the CRT is shown in **Fig. 10**. The position of the present operating point on a capability curve of the generator is displayed.

4. Results of Verification and Test

4.1 Magnetic field in the end zone of the stator core

First, three dimensional magnetic field analysis using the finite element method was performed to verify various countermeasures in the above-mentioned **Table 3**. **Table 5** shows these calculation results. Leakage flux in the end zone was measured by the shop test as well as by the on-site

Table 5 Comparison of flux, generated loss and temperature at rated apparent load, power factor 0.95 leading

Item	Flux shield			
	with		without	
	Slit in teeth		Slit in teeth	
	with	without	with	without
Max. flux density at tooth top (T)	0.494	0.494	0.735	0.735
Eddy current loss (W/cm^2)	4,300	7,300	9,450	16,200
Temp. rise (K)	36	56	60	134

Table 6 Comparison of values between analyzed and measured on the leakage flux at the stator core end

Condition	Position	Flux density (T)	
		Analyzed	Measured
No load, rated voltage	Tooth center	0.090	0.093
3-phase short circuit, rated current		0.210	0.208
450MW, 120Mvar leading		0.190	0.180
600MW, 100Mvar leading		0.220	0.210
670MVA, p.f. 0.95 leading	Tooth top	0.494	(0.474)*

* Exterpolated value from measured values up to 600MW, leading 100Mvar

Fig. 12 Result of loss reduction measures

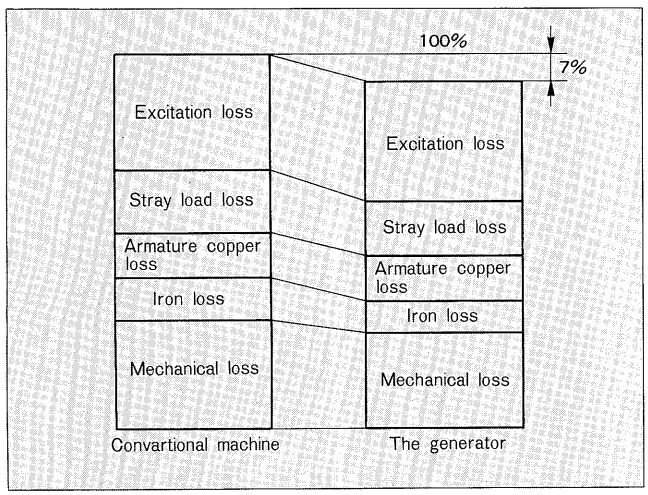

Table 7 Measured shaft vibration

unit; μm (p-p)

Generator load	No. of journal bearing		
	#6	#7	#8
No load	24	14	25
300MW	30	7	18
600MW	40	13	20

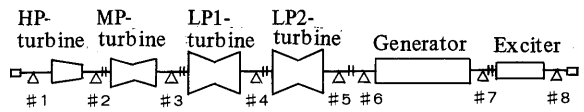

Fig. 13 Induced voltage wave-forms of layer monitor search coil

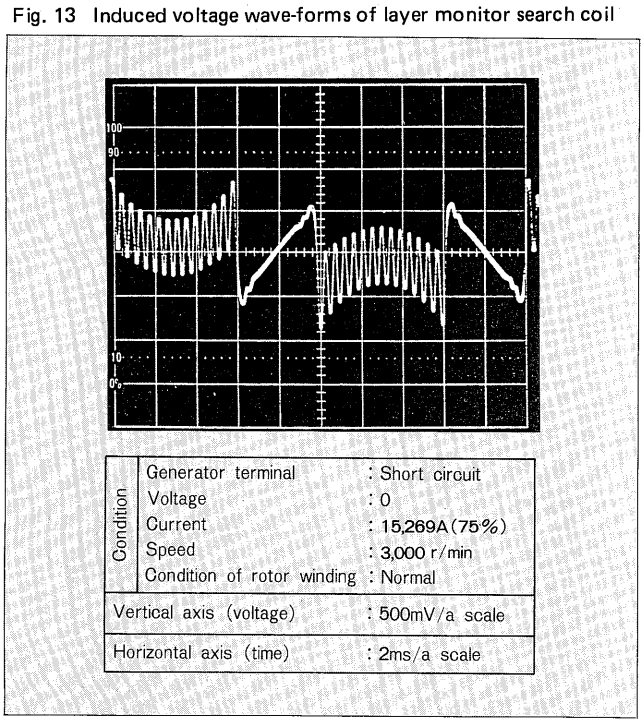

test for verification. The results of the analysis and measurement concurred, and the effectiveness of the flux shield ring and tooth slit applied to this generator is shown in **Table 6**.

4.2 No-load saturation characteristic and 3 phase short circuit characteristic

Figure 11 shows the measurement results.

4.3 Generator loss and temperature rise

The losses of this generator as compared with a conventional machine are shown in **Fig. 12**. Among these losses, reductions are seen in mechanical loss and iron loss. The reduction of mechanical loss is an effect of the decrease in the quantity of excessive gas, which is directly related to the appropriate distribution of the cooling gas. The reduction of iron loss is due to the improvement of the core plate material.

The winding's rises in temperature at rated load were

(1) Stator winding: 43.2 K, and
(2) Rotor winding: 40.2 K.

4.4 Vibration

Table 7 shows the measurement results of shaft vibration of the generator and exciter, which are directly coupled with the turbine. These were excellent results at all bearings against the control value of 50 μm (p-p).

4.5 Layer short detection in rotor

Induced voltage wave form of the rotor slot under normal conditions was measured and recorded by layer short detection equipment[1] in the shop test for use in future protective maintenance of the rotor. **Fig. 13** shows the waveform.

5. Conclusion

Unit 1 Steam Turbine Generator of Noshiro Thermal Power Plant smoothly passed the commissioning test and began commercial operation in May 1993. To ensure high reliability of Fuji Electric's maximum capacity generator, quality control over each step of design, manufacture, assembly and test has been performed. These valuable results and experiences obtained through these processes will be utilized to develop future technology.

The authors would like to express appreciation to the related engineers of Tohoku Electric Power Co., Inc. for guidance in the manufacturing of this generator.

Reference:

(1) S. Moriyasu, I. Miura, T. Kobaru: Advanced Technology of Turbine Generator, Fuji Electric Review, Vol. 33, No. 3, p. 107–112 (1987)